Al-Furat Journal of Innovations in Agricultural Sciences (FJIAS)
ISSN: 2789-6773 | https://doi.org/10.46649/fjias.v2.si1.18
Vol. 2, Special Issue 1 (2026): ICSDCC 2026 – 3rd International Conference on Sustainable Development and Climate Change

THERMAL–HYDRAULIC AND NET-ENERGY ASSESSMENT OF TRANSVERSE BAFFLES IN A NARROW REAR AIR CHANNEL FOR COOLING THE PHOTOVOLTAIC ARRAYS OF SOLAR IRRIGATION PUMPING SYSTEMS IN HOT CLIMATES

Jaber Ali Zghair[1*]

[1]Al-Mussaib Technical College, Al-Furat Al-Awsat Technical University, 51009 Babylon, Iraq

*Corresponding author E-mail: jaber.aass@atu.edu.iq

Accepted 20/11/2026, Available online 20/11/2026

FJIAS 2026, 2(SI 1): Article 18

Abstract. *Solar photovoltaic (PV) water pumping is spreading rapidly in Iraqi agriculture, but the electrical output of PV arrays, and hence the volume of irrigation water pumped, falls as module temperature rises during the hot summer months when crop water demand peaks. Forced air flow through a narrow channel behind the module is a low-cost, water-free way to limit cell temperature, and transverse baffles are often proposed to intensify it. Baffles are normally judged with the equal-pumping-power criterion PEC = $(Nu/Nu_0)/(f/f_0)^{1/3}$, which was derived for heat exchangers and does not account for the electrical value of a lower PV temperature. This study simulates laminar forced convection (Re = 100–600, Pr = 0.71) in a parallel-plate channel whose upper wall receives a uniform heat flux from the PV rear surface, with adiabatic baffles mounted on the opposite, insulated wall. The baffle blockage ratio (e/H = 0.3–0.7) and number (n = 3, 5, 7 over a heated length of 10H) were varied in 40 cases. The stream function–vorticity equations were solved with a conservative TVD finite-volume scheme. The solver reproduces the exact fully developed Nusselt number (5.385) and the analytical energy balance within 1.4%. Baffles raised Nu by 12–148% and lowered the maximum heated-wall temperature by 5–49%, but the friction factor rose by a factor of 1.6–38, so that PEC remained between 0.67 and 0.96 in every case. In contrast, a net-energy analysis for a 5 mm channel under Baghdad summer conditions shows that the electrical gain from the lower module temperature exceeds the additional fan power in all 36 baffled cases. The largest net gain (9.8 W m^{-2}, 5.4% of the reference output) was obtained with the highest blockage at Re = 100, whereas at Re = 600 a moderate blockage (e/H = 0.5) was best (2.9 W m^{-2}). Correlations for Nu and f are proposed (mean deviations 2.7% and 3.7%). The conventional PEC can therefore reject baffle designs that are energetically beneficial for cooling the PV arrays of solar irrigation pumps, and the optimum blockage decreases as the flow rate increases.*

Keywords: *solar irrigation pumping; photovoltaic cooling; baffled channel; laminar forced convection; net power gain; hot climate*

This article is published under the terms of the **Creative Commons Attribution 4.0 International License (CC BY 4.0)**, which permits unrestricted use, distribution, and reproduction in any medium, provided the original work is properly cited.

Al-Furat Journal of Innovations in Agricultural Sciences (FJIAS)
ISSN: 2789-6773 | https://doi.org/10.46649/fjias.v2.si1.18
Vol. 2, Special Issue 1 (2026): ICSDCC 2026 – 3rd International Conference on Sustainable Development and Climate Change

NOMENCLATURE

Symbol	Description
D_h	hydraulic diameter, $2H$ (m)
e	baffle height (m)
f	Darcy friction factor of the heated section, Eq. (6)
G	solar irradiance (W m^{-2})
H	channel height (m)
k	air thermal conductivity (W m^{-1} K^{-1})
L_h	heated length, $10H$ (m)
n	number of baffles
Nu	average Nusselt number, Eq. (5)
P	baffle pitch, L_h/n (m)
PEC	performance evaluation criterion, Eq. (7)
Pr	Prandtl number
q''	heat flux from the PV rear surface (W m^{-2})
Re	Reynolds number, $\bar{U}\,D_h/\nu$
Ri_q	flux-based Richardson number, Eq. (9)
$\bar{U}$	mean velocity (m s^{-1})
β_{PV}	temperature coefficient of PV efficiency (K^{-1})
η_{ref}, η_{fan}	reference PV efficiency; fan efficiency
θ	dimensionless temperature, $(T - T_{in})/(q''H/k)$
ψ, ω	dimensionless stream function and vorticity
Subscripts	*w* wall; *b* bulk; 0 smooth channel at the same Re

1. INTRODUCTION

The electrical efficiency of crystalline silicon PV modules falls almost linearly with cell temperature, typically by 0.4–0.5% per kelvin [1,2]. The penalty is severe in Iraq, where summer ambient temperatures exceed 45 °C. Field measurements in Baghdad recorded cell temperatures of 45–65 °C and a power temperature coefficient of −0.52% K^{-1} for a polycrystalline module [3], and module temperatures up to 81 °C have been reported in August [4]. Cooling the module is therefore a direct way to recover electrical output, and many active and passive techniques have been tested under Iraqi conditions, including underground-water cooling [5], water sprays and rear-side fins [4].

The penalty matters particularly for agriculture. PV water pumping has become an established alternative to diesel and grid-powered pumps for irrigating isolated farms in Iraq: direct-coupled PV pumps have been designed to supply sprinkler-irrigated greenhouses from deep wells [6], PV well-pumping systems have been implemented and recommended for Iraqi conditions [7], and optimal PV array sizing for small-scale irrigation has been studied for the Samarra region [8]. In such systems the pumped water volume follows the array output, so the drop in module efficiency during the hottest months coincides with the period of highest crop water demand. Because water is scarce on these farms, water-based module cooling is undesirable, and air cooling becomes the natural option.

Air cooling through a channel behind the module is attractive where water is scarce. Passive (buoyancy-driven) channels are simple but limited by the low heat transfer coefficient of air [9–11]; El Kharaz et al. [10] reported mean wall temperatures of about 358 K in a 15

This article is published under the terms of the **Creative Commons Attribution 4.0 International License (CC BY 4.0)**, which permits unrestricted use, distribution, and reproduction in any medium, provided the original work is properly cited.

Al-Furat Journal of Innovations in Agricultural Sciences (FJIAS)
ISSN: 2789-6773 | https://doi.org/10.46649/fjias.v2.si1.18
Vol. 2, Special Issue 1 (2026): ICSDCC 2026 – 3rd International Conference on Sustainable Development and Climate Change

mm channel at 300 W m^{-2}. A small fan increases heat removal, and disturbing the boundary layer with baffles or ribs can increase it further. Baffled channels have been studied extensively for heat exchangers and solar air heaters since the periodic laminar analysis of Kelkar and Patankar [12]; they were reviewed recently by Henniche and Korichi [13], and three-dimensional baffle geometries continue to be investigated [14]. In PV cooling, baffles have been combined with nanofluids [15] and semicircular baffles have been used in water-based PV/T channels [16]. Lima-Téllez et al. [15] found that baffles improved electrical efficiency by about 2%, and Altharwanee et al. [16] reported Nu increases of 32–132% together with friction increases of 22–96%.

Most such studies rank baffle configurations with the performance evaluation criterion PEC = $(Nu/Nu_0)/(f/f_0)^{1/3}$, which measures heat transfer at equal pumping power [17,18]. This criterion was devised for heat exchangers, in which pumping power and heat duty have comparable economic value. In PV cooling, however, the useful product is electricity: each kelvin of temperature reduction is worth a definite electrical power, and the fan power is small compared with the module output. A design with PEC < 1 may therefore still increase the net electrical output. To the author's knowledge, the PEC ranking and a direct net-energy ranking have not been compared systematically for baffled PV cooling channels, and the effect of baffle blockage and number on the outcome has not been documented for the laminar regime typical of narrow (millimetre-scale) rear channels.

This study addresses that gap with a numerical parametric analysis of a narrow rear air channel with transverse baffles mounted on the insulated wall, so that the PV laminate itself is not modified. The contributions are: (i) a verified dataset of 40 laminar solutions covering three blockage ratios, three baffle numbers and four Reynolds numbers; (ii) a comparison between the PEC criterion and a net-power criterion based on the PV temperature coefficient, evaluated for Baghdad summer conditions representative of solar irrigation pumping sites in central Iraq; and (iii) correlations for Nu and f for design use.

2. PROBLEM FORMULATION

2.1. Physical model and assumptions

The computational domain (Fig. 1) is a two-dimensional parallel-plate channel of height H that represents the air gap between the PV rear surface and an insulated back plate. The upper wall is heated by a uniform flux q'' over a length $L_h = 10H$; the upstream ($2H$) and downstream ($15H$) extensions are adiabatic. The long outlet extension keeps the recirculation behind the last baffle away from the outflow boundary. n thin baffles (thickness $0.1H$, height e) are attached to the insulated lower wall at equal pitch $P = L_h/n$, starting at $P/2$ from the leading edge of the heated section. Mounting the baffles on the insulated wall deflects the flow towards the PV surface without bonding anything to the module. The baffles are adiabatic (e.g. polymer). The flow is laminar, incompressible and two-dimensional with constant properties. Buoyancy, radiation and conduction in the PV laminate are neglected; the validity of neglecting buoyancy is checked in Section 5.

This article is published under the terms of the **Creative Commons Attribution 4.0 International License (CC BY 4.0)**, which permits unrestricted use, distribution, and reproduction in any medium, provided the original work is properly cited.

Al-Furat Journal of Innovations in Agricultural Sciences (FJIAS)
ISSN: 2789-6773 | https://doi.org/10.46649/fjias.v2.si1.18
Vol. 2, Special Issue 1 (2026): ICSDCC 2026 – 3rd International Conference on Sustainable Development and Climate Change

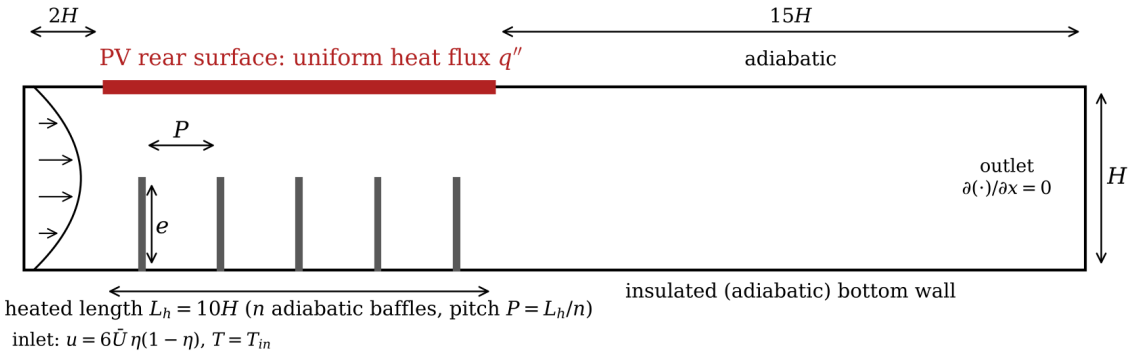


Fig. 1. Computational domain and boundary conditions (vertical scale exaggerated three times). The case shown has $n = 5$ and $e/H = 0.5$.

2.2. Governing equations

With H, the mean velocity $\bar{U}$ and $H/\bar{U}$ as scales and $\theta = (T - T_{in})/(q''H/k)$, the stream function–vorticity form of the equations is

$$U = \partial\psi/\partial Y,\ \ V = -\partial\psi/\partial X,\ \ \nabla^2\psi = -\omega \tag{1}$$

$$\partial\omega/\partial\tau + \nabla\cdot(\mathbf{u}\omega) = (2/\mathrm{Re})\,\nabla^2\omega \tag{2}$$

$$\partial\theta/\partial\tau + \nabla\cdot(\mathbf{u}\theta) = [2/(\mathrm{Re\ Pr})]\,\nabla^2\theta \tag{3}$$

where $\mathrm{Re} = \bar{U}D_h/\nu$ with $D_h = 2H$. The boundary conditions are: a fully developed inlet profile $U = 6Y(1 - Y)$, $\psi = Y^2(3 - 2Y)$, $\theta = 0$; zero streamwise gradients at the outlet; no slip on all walls and baffles, with $\psi = 0$ on the lower wall and baffles and $\psi = 1$ on the upper wall; $\partial\theta/\partial Y = 1$ on the heated part of the upper wall; and zero heat flux on all other surfaces.

2.3. Performance parameters

The bulk temperature and the average Nusselt number over the heated section are

$$\theta_b(X) = \int_0^1 U\theta\,dY \,/\, \int_0^1 U\,dY \tag{4}$$

$$\mathrm{Nu} = q''D_h/[k(\bar{T}_w - \bar{T}_b)] = 2/(\bar{\theta}_w - \bar{\theta}_b) \tag{5}$$

where the overbar denotes the average over L_h. On the flat heated wall the X-momentum equation reduces to $\partial p/\partial X = -(2/\mathrm{Re})\,\partial\omega/\partial Y$, so the pressure drop is obtained by integrating the wall vorticity gradient along the whole channel. Because the inlet and outlet flows are fully developed, the wall pressure equals the cross-sectional pressure there. The friction factor attributed to the heated (baffled) section is

$$f = 2\Delta p_h D_h/(\rho\bar{U}^2 L_h),\ \ \Delta p_h = \Delta p_{total} - \Delta p_0(L - L_h) \tag{6}$$

where Δp_0 is the fully developed smooth-channel pressure gradient, so that the losses in the outlet recovery zone are charged to the baffles that cause them. The equal-pumping-power criterion [17,18] is

$$\mathrm{PEC} = (\mathrm{Nu}/\mathrm{Nu}_0)\,/\,(f/f_0)^{1/3} \tag{7}$$

This article is published under the terms of the **Creative Commons Attribution 4.0 International License (CC BY 4.0)**, which permits unrestricted use, distribution, and reproduction in any medium, provided the original work is properly cited.

Al-Furat Journal of Innovations in Agricultural Sciences (FJIAS)
ISSN: 2789-6773 | https://doi.org/10.46649/fjias.v2.si1.18
Vol. 2, Special Issue 1 (2026): ICSDCC 2026 – 3rd International Conference on Sustainable Development and Climate Change

3. NUMERICAL METHOD AND VERIFICATION

3.1. Solution procedure

Equations (2) and (3) were discretised on a uniform vertex-centred grid in conservative finite-volume form. Convective face values were reconstructed with a second-order TVD scheme with the van Leer limiter [20], and face velocities were computed from ψ so that the discrete continuity equation is satisfied exactly in each control volume. Diffusion used second-order central differences. For the energy equation, convective and diffusive fluxes through all solid faces were set to zero except at the heated wall, where the exact flux was imposed, so the discrete energy balance is conservative. The Poisson equation (1) was solved at every pseudo-time step with a sparse direct LU factorisation. Wall vorticity followed Thom's formula, averaged at baffle corners. The equations were marched explicitly in pseudo-time with an adaptive step from the combined convective–diffusive stability limit until the maximum rate of change of θ fell below 10^{-5}, and for at least three flow-through times. All 40 cases reached a steady state, and no vortex shedding occurred in the present range. The heated-wall temperature was evaluated with a second-order one-sided expression. The code was written in Python with Numba compilation.

3.2. Verification

Three analytical checks were used. (i) For the smooth channel the computed *f*Re was 94.7 on the production grid (95.0 with 40 cells per *H*), against the exact value of 96 (−1.4% and −1.0%). (ii) At Re = 20 (Pe = 14.2), the local Nusselt number in the thermally developed part of the heated section ($X - X_0$ = 4–9) was 5.380–5.385, against the exact fully developed value of 5.385 for a parallel-plate channel with one wall at uniform flux and the other insulated [19]. (iii) The bulk temperature rise across the heated section agreed with the energy balance $\theta_{b,out} = 2L_h/(\mathrm{Re}\,\mathrm{Pr}\,H)$ within 1.4% in all cases, including the most blocked ones.

Table 1 summarises the grid study. Nu changes by less than 1.3% between 30 and 40 cells per *H*. The friction factor is more sensitive because of the singular flow at the sharp baffle tips: the change is 2.3% at e/H = 0.5 and 11% at e/H = 0.7, Re = 600. The production grid (30 cells per *H*, 811 × 31 nodes) therefore underestimates *f* for the most blocked cases at the highest Re, and the fan-power estimates for these cases are lower bounds. This does not affect the conclusions, since these cases already have the lowest PEC and the smallest net gain.

Table 1. Grid sensitivity of Nu and *f*Re.

Case	Cells per *H*	Nu	*f*Re	$\theta_{w,max}$
Smooth, Re = 600	30 / 40	9.163 / 9.182	94.5 / 95.0	0.325 / 0.325
n = 5, e/H = 0.5, Re = 200	30 / 40	11.099 / 11.173	576.1 / 580.7	0.348 / 0.349
n = 5, e/H = 0.5, Re = 600	20 / 30 / 40	14.478 / 14.556 / 14.726	743.4 / 802.3 / 820.9	0.224 / 0.220 / 0.219
n = 7, e/H = 0.7, Re = 600	30 / 40	21.085 / 21.358	3558 / 3978	0.165 / 0.162

This article is published under the terms of the **Creative Commons Attribution 4.0 International License (CC BY 4.0)**, which permits unrestricted use, distribution, and reproduction in any medium, provided the original work is properly cited.

Al-Furat Journal of Innovations in Agricultural Sciences (FJIAS)
ISSN: 2789-6773 | https://doi.org/10.46649/fjias.v2.si1.18
Vol. 2, Special Issue 1 (2026): ICSDCC 2026 – 3rd International Conference on Sustainable Development and Climate Change

4. RESULTS AND DISCUSSION

4.1. Flow and thermal fields

Fig. 2 shows streamlines and isotherms at Re = 600. In the smooth channel a thermal boundary layer grows along the heated wall and the wall temperature rises continuously. Baffles on the opposite wall form recirculation cells between them and push the core flow towards the heated wall. With e/H = 0.3 the deflection is weak and the thermal boundary layer is only thinned. With e/H = 0.5 the main stream follows the heated wall through the gap above each baffle; with e/H = 0.7 the flow passes through a gap of 0.3H at about three times the mean velocity, and the cells fill the whole inter-baffle space. The thinned thermal boundary layer is the main mechanism of enhancement; the recirculation cells themselves stay at nearly inlet temperature because they are bounded by adiabatic surfaces. Increasing n from 5 to 7 at e/H = 0.5 changes the field little, because the main stream already remains attached to the heated wall between baffles.

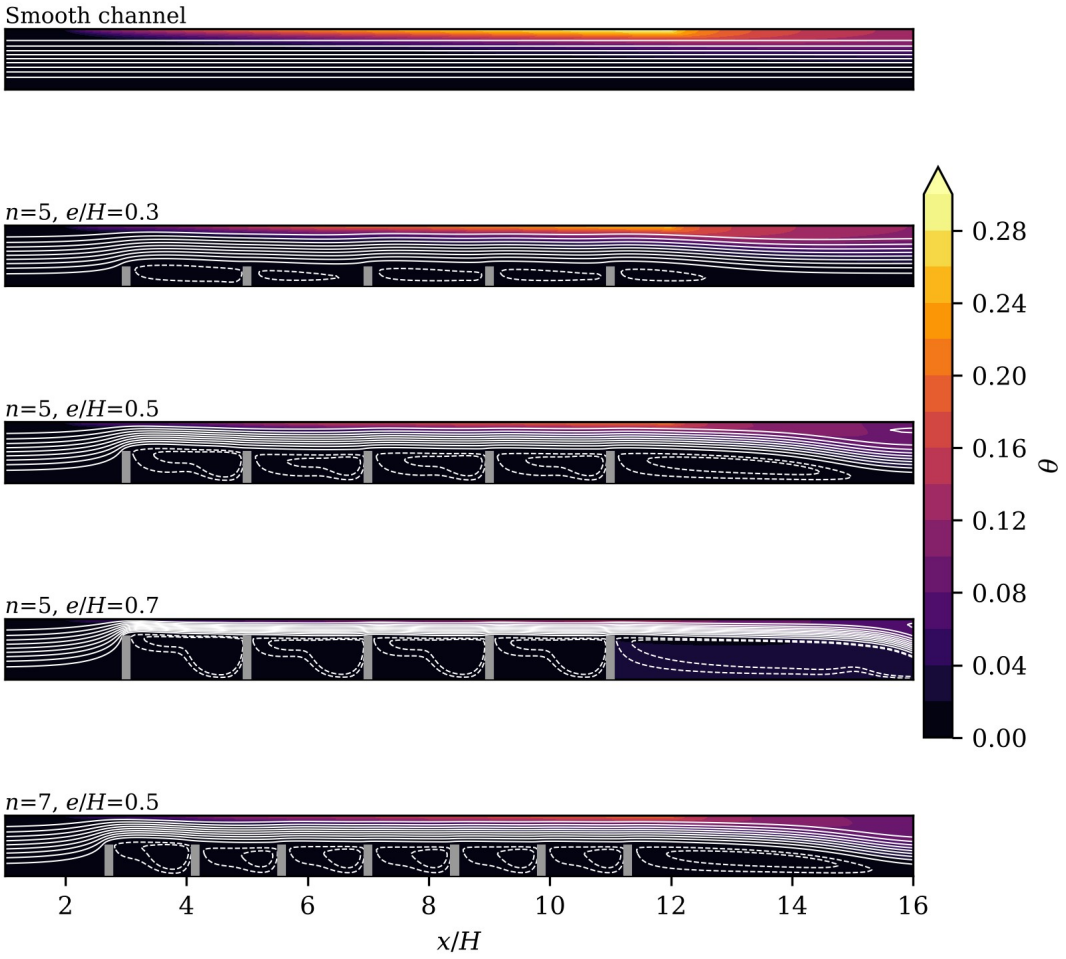


Fig. 2. Isotherms (colour) and streamlines (white; dashed lines are recirculating) at Re = 600 for the smooth channel and selected baffle arrangements, from X = 1 to 16.

This article is published under the terms of the **Creative Commons Attribution 4.0 International License (CC BY 4.0)**, which permits unrestricted use, distribution, and reproduction in any medium, provided the original work is properly cited.

Al-Furat Journal of Innovations in Agricultural Sciences (FJIAS)
ISSN: 2789-6773 | https://doi.org/10.46649/fjias.v2.si1.18
Vol. 2, Special Issue 1 (2026): ICSDCC 2026 – 3rd International Conference on Sustainable Development and Climate Change

The heated-wall temperature distributions in Fig. 3 show the practical effect. At Re = 600 the smooth channel reaches $\theta_{w,max}$ = 0.325 at the end of the heated section; five baffles with e/H = 0.5 reduce it to 0.220 (−32%) and with e/H = 0.7 to 0.167 (−49%). Local minima appear just downstream of each gap, where the accelerated stream approaches the wall. At Re = 200 the reductions are similar in relative terms, but the absolute temperatures are higher because the bulk temperature rise is three times larger.

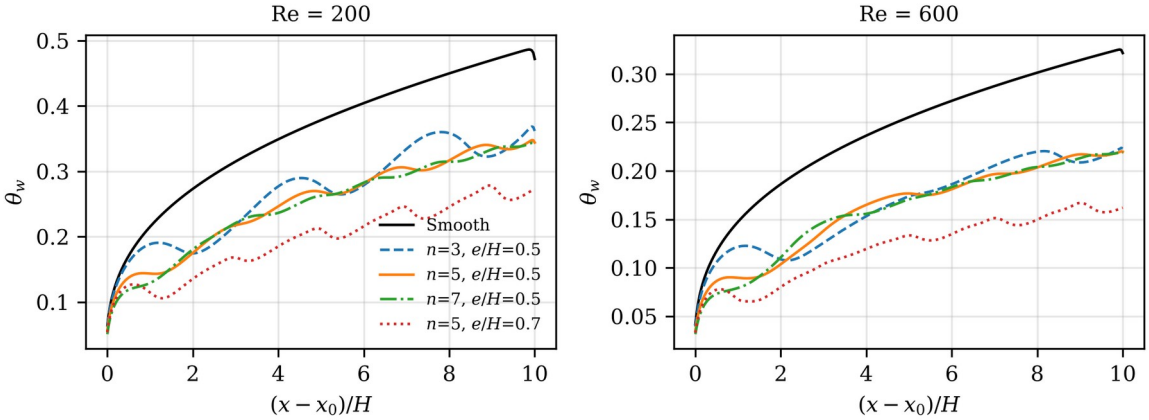


Fig. 3. Dimensionless heated-wall temperature along the heated section at (a) Re = 200 and (b) Re = 600.

4.2. Heat transfer, friction and PEC

The integral results are given in Fig. 4 and Table 2. Blockage is the dominant parameter. Nu/Nu_0 lies between 1.12 and 1.27 for e/H = 0.3, 1.35 and 1.65 for e/H = 0.5, and 1.79 and 2.48 for e/H = 0.7. The number of baffles has a secondary effect that weakens as Re increases: increasing n from 3 to 7 raises Nu by 11–38% at Re = 100 but by only 3.5–9% at Re = 600. With n = 3, Nu/Nu_0 increases with Re because the recirculation zones grow and deflect the stream over a larger part of the pitch. With n = 7, Nu/Nu_0 decreases slightly with Re because the smooth-channel Nu_0 itself increases with Re in the developing region.

The friction penalty grows much faster than the heat transfer. f/f_0 ranges from 1.6 (n = 3, e/H = 0.3, Re = 100) to 37.7 (n = 7, e/H = 0.7, Re = 600), and it rises with Re because form drag, which scales with $\rho\bar{U}^2$, replaces viscous friction, which scales with $\mu\bar{U}$. As a result, PEC is below unity in all 36 cases (0.67–0.96). It decreases with blockage and with Re and is nearly independent of n. By the equal-pumping-power criterion, then, no baffle configuration in this range would be recommended. This agrees with the general observation that laminar baffled channels rarely achieve PEC > 1 without vortex-generating geometries [12,13].

This article is published under the terms of the **Creative Commons Attribution 4.0 International License (CC BY 4.0)**, which permits unrestricted use, distribution, and reproduction in any medium, provided the original work is properly cited.

Al-Furat Journal of Innovations in Agricultural Sciences (FJIAS)
ISSN: 2789-6773 | https://doi.org/10.46649/fjias.v2.si1.18
Vol. 2, Special Issue 1 (2026): ICSDCC 2026 – 3rd International Conference on Sustainable Development and Climate Change

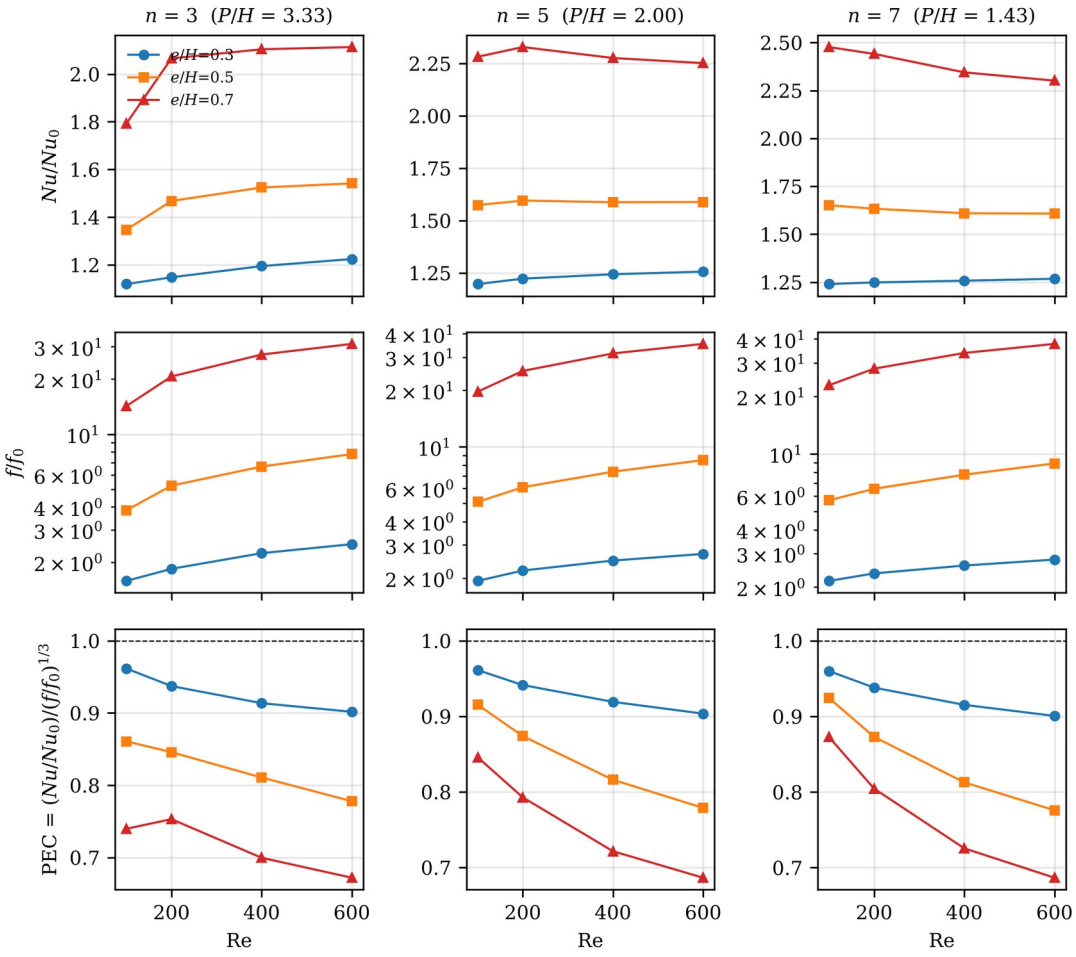


Fig. 4. Nusselt number ratio (top), friction factor ratio (middle, logarithmic scale) and PEC (bottom) versus Re for n = 3, 5 and 7.

5. NET-ENERGY ASSESSMENT FOR THE PV ARRAY OF A SOLAR IRRIGATION PUMP

To assess the baffles by their effect on PV output, the dimensionless results were applied to a representative design: H = 5 mm (D_h = 10 mm), air at 45 °C (ρ = 1.109 kg m^{-3}, ν = 1.75 × 10^{-5} m^2 s^{-1}, k = 0.0274 W m^{-1} K^{-1}), a rear heat flux q'' = 300 W m^{-2} (the upper value used in [10]), G = 1000 W m^{-2}, η_{ref} = 0.18, β_{PV} = 0.0052 K^{-1} (measured in Baghdad [3]) and a small-fan efficiency η_{fan} = 0.3. Re = 100–600 then corresponds to $\bar{U}$ = 0.18–1.05 m s^{-1}. Baffles mainly reduce the wall-to-bulk temperature difference; the bulk temperature rise, which depends only on the flow rate, is unchanged. The reduction in the mean module temperature and the resulting electrical gain per unit module area are

$$\Delta T = (q''D_h/k)(1/\mathrm{Nu}_0 - 1/\mathrm{Nu}),\quad \Delta P_{el} = G\eta_{ref}\beta_{PV}\Delta T \tag{8}$$

and the additional fan power per unit module area, together with the flux-based Richardson number, are

$$\Delta P_{fan} = (\Delta p_h - \Delta p_{h,0})\bar{U}H/(\eta_{fan}L_h),\quad \mathrm{Ri}_q = [g\beta q''H^4/(k\nu^2)]/(\mathrm{Re}/2)^2 \tag{9}$$

This article is published under the terms of the **Creative Commons Attribution 4.0 International License (CC BY 4.0)**, which permits unrestricted use, distribution, and reproduction in any medium, provided the original work is properly cited.

Al-Furat Journal of Innovations in Agricultural Sciences (FJIAS)
ISSN: 2789-6773 | https://doi.org/10.46649/fjias.v2.si1.18
Vol. 2, Special Issue 1 (2026): ICSDCC 2026 – 3rd International Conference on Sustainable Development and Climate Change

For this design Ri_q = 0.28, 0.07, 0.02 and 0.008 at Re = 100, 200, 400 and 600, so the forced-convection assumption is well satisfied for Re ≥ 200 and acceptable at Re = 100, where heating from above (a stably stratified layer) further limits buoyancy-driven mixing.

Fig. 5 shows the results. The temperature reduction ranges from 1.9 K (n = 3, e/H = 0.3, Re = 100) to 10.6 K (n = 7, e/H = 0.7, Re = 100), giving electrical gains of 1.8–9.9 W m^{-2}, i.e. 1.0–5.5% of the 180 W m^{-2} reference output. The additional fan power is two to three orders of magnitude smaller at low Re (0.003–0.10 W m^{-2} at Re = 100) but grows roughly with $\bar{U}^3$, reaching 5.1–6.2 W m^{-2} for e/H = 0.7 at Re = 600. The net gain is positive in all 36 cases, although every one of them has PEC < 1. The ranking also differs from the PEC ranking. At Re = 100 and 200 the most blocked and densest arrangement (n = 7, e/H = 0.7) gives the largest net gain (9.8 and 8.2 W m^{-2}), whereas it has the lowest PEC in its row. At Re = 600 the net gain of the e/H = 0.7 baffles falls to 0.15–0.82 W m^{-2}, and the moderate blockage e/H = 0.5 becomes optimal (2.8–2.9 W m^{-2}). The optimum blockage therefore decreases as the flow rate rises. A designer can reach a given module temperature either with a faster smooth-channel flow or with baffles at a lower flow rate, and the second option is clearly preferable: highly blocked baffles at Re = 100–200 give larger temperature reductions than a smooth channel at Re = 600, for a fraction of the fan power.

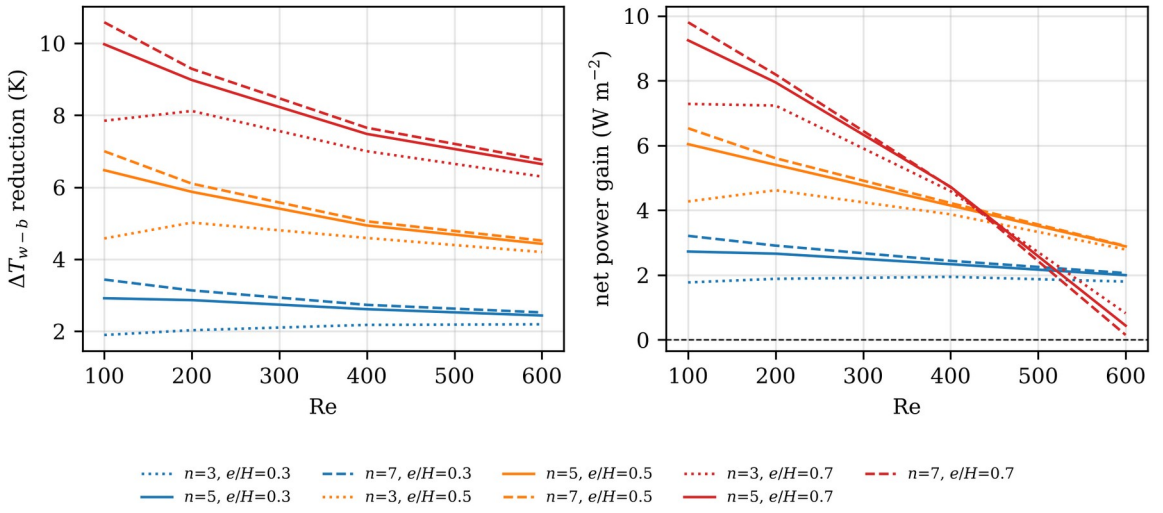


Fig. 5. Application to a 5 mm channel under Baghdad summer conditions: (a) reduction in mean module temperature relative to the smooth channel; (b) net power gain (electrical gain minus additional fan power).

The PEC criterion is too conservative here because it compares heat transfer at equal pumping power, implicitly valuing pumping energy as highly as the heat transferred. In PV cooling, one kelvin of module temperature is worth about $G\eta_{ref}\beta_{PV} \approx 0.94$ W m^{-2}, while the fan power in narrow laminar channels is of the order of 0.01–1 W m^{-2}. Net power, or an equivalent criterion that weights fan power against the electrical value of the temperature reduction, is the appropriate design metric.

For a solar irrigation pump, the net electrical gain of 1–5% of the reference output is available during the hottest hours of the hottest months, when module temperatures are highest and crop water demand peaks. In a direct-coupled PV pumping system [6] the additional array power increases the daily pumped volume, although not strictly in proportion,

This article is published under the terms of the **Creative Commons Attribution 4.0 International License (CC BY 4.0)**, which permits unrestricted use, distribution, and reproduction in any medium, provided the original work is properly cited.

Al-Furat Journal of Innovations in Agricultural Sciences (FJIAS)
ISSN: 2789-6773 | https://doi.org/10.46649/fjias.v2.si1.18
Vol. 2, Special Issue 1 (2026): ICSDCC 2026 – 3rd International Conference on Sustainable Development and Climate Change

because pump flow depends non-linearly on input power and on the pump–array matching. Because the fan can be supplied directly by the array, the cooling channel adds no external energy demand and no water consumption. Quantifying the gain in pumped water for a specific pump, head and irrigation schedule requires a coupled array–pump model and is recommended for future work.

Table 2. Integral results for the baffled channels (30 cells per H).

Re	n	e/H	Nu	Nu/Nu$_0$	f/f_0	PEC	$\Delta\theta_{max}$ (%)	ΔT (K)	Net gain (W m^{-2})
100	3	0.3	6.91	1.120	1.58	0.961	5.0	1.89	1.77
100	3	0.5	8.31	1.347	3.84	0.861	14.5	4.58	4.27
100	3	0.7	11.06	1.792	14.23	0.740	27.0	7.85	7.28
100	5	0.3	7.38	1.197	1.93	0.961	9.7	2.91	2.72
100	5	0.5	9.71	1.574	5.08	0.915	21.9	6.47	6.04
100	5	0.7	14.08	2.282	19.64	0.846	33.8	9.97	9.24
100	7	0.3	7.65	1.240	2.15	0.960	11.2	3.43	3.21
100	7	0.5	10.19	1.651	5.70	0.924	23.5	7.00	6.53
100	7	0.7	15.28	2.476	22.85	0.873	34.9	10.58	9.80
200	3	0.3	7.99	1.148	1.84	0.937	8.4	2.03	1.88
200	3	0.5	10.21	1.468	5.23	0.846	24.2	5.02	4.62
200	3	0.7	14.37	2.066	20.64	0.753	40.5	8.12	7.23
200	5	0.3	8.51	1.222	2.19	0.941	13.2	2.86	2.66
200	5	0.5	11.10	1.595	6.08	0.874	28.5	5.87	5.40
200	5	0.7	16.20	2.328	25.34	0.793	42.8	8.98	7.95
200	7	0.3	8.69	1.249	2.36	0.938	14.2	3.13	2.91
200	7	0.5	11.36	1.633	6.55	0.873	29.4	6.10	5.60
200	7	0.7	16.98	2.441	27.92	0.804	43.8	9.29	8.19
400	3	0.3	9.81	1.195	2.24	0.914	12.7	2.18	1.94
400	3	0.5	12.51	1.524	6.65	0.811	29.6	4.59	3.87
400	3	0.7	17.26	2.104	27.19	0.700	45.7	7.00	4.59
400	5	0.3	10.20	1.243	2.48	0.919	15.4	2.61	2.33
400	5	0.5	13.03	1.587	7.36	0.816	31.4	4.94	4.14
400	5	0.7	18.68	2.276	31.40	0.721	47.2	7.48	4.72
400	7	0.3	10.32	1.257	2.59	0.915	15.8	2.73	2.44
400	7	0.5	13.21	1.609	7.77	0.813	31.8	5.05	4.22
400	7	0.7	19.24	2.344	33.74	0.725	48.1	7.65	4.71
600	3	0.3	11.22	1.224	2.51	0.902	15.1	2.19	1.80
600	3	0.5	14.12	1.541	7.78	0.778	31.2	4.20	2.79
600	3	0.7	19.36	2.113	31.10	0.672	47.7	6.29	0.82
600	5	0.3	11.51	1.256	2.69	0.903	16.4	2.44	2.00
600	5	0.5	14.56	1.589	8.49	0.779	32.3	4.43	2.88
600	5	0.7	20.63	2.252	35.30	0.686	48.7	6.64	0.44
600	7	0.3	11.61	1.267	2.79	0.901	16.6	2.52	2.06
600	7	0.5	14.73	1.608	8.90	0.776	32.6	4.52	2.90
600	7	0.7	21.09	2.301	37.65	0.687	49.4	6.76	0.15

$\Delta\theta_{max}$: reduction of the maximum heated-wall temperature relative to the smooth channel; ΔT and net gain: application of Section 5. Smooth-channel reference values: Re = 100: Nu$_0$ = 6.169, f_0Re = 94.7; Re = 200: Nu$_0$ = 6.958, f_0Re = 94.7; Re = 400: Nu$_0$ = 8.207, f_0Re = 94.6; Re = 600: Nu$_0$ = 9.163, f_0Re = 94.5.

6. CORRELATIONS

For design use, the 36 baffled-channel results were fitted by least squares ($100 \le \mathrm{Re} \le 600$, $0.3 \le e/H \le 0.7$, $1.43 \le P/H \le 3.33$, Pr = 0.71, $L_h = 10H$):

$$\ln \mathrm{Nu} = 0.788 + 0.242 \ln \mathrm{Re} + 0.045 \ln(e/H) - 0.666 \ln(1 - e/H) - 0.136 \ln(P/H) \quad (10)$$

This article is published under the terms of the **Creative Commons Attribution 4.0 International License (CC BY 4.0)**, which permits unrestricted use, distribution, and reproduction in any medium, provided the original work is properly cited.

Al-Furat Journal of Innovations in Agricultural Sciences (FJIAS)
ISSN: 2789-6773 | https://doi.org/10.46649/fjias.v2.si1.18
Vol. 2, Special Issue 1 (2026): ICSDCC 2026 – 3rd International Conference on Sustainable Development and Climate Change

$$\ln f = 4.373 - 0.847 \ln \mathrm{Re} + 0.438 \ln(e/H) - 1.511 \ln(1 - e/H) - 0.289 \ln(P/H) - 0.171 \ln \mathrm{Re} \cdot \ln(1 - e/H) \quad (11)$$

Eq. (10) gives R^2 = 0.986, a mean absolute deviation of 2.7% and a maximum deviation of 12.8%; Eq. (11) gives R^2 = 0.991, 3.7% and 14.6%, respectively (Fig. 6). The largest deviations occur for n = 3 at Re = 100, where the developing inlet flow cannot be represented by the power-law form. The terms in ln(1 − e/H) represent flow acceleration in the gap above the baffles, which dominates both Nu and f at high blockage ratios.

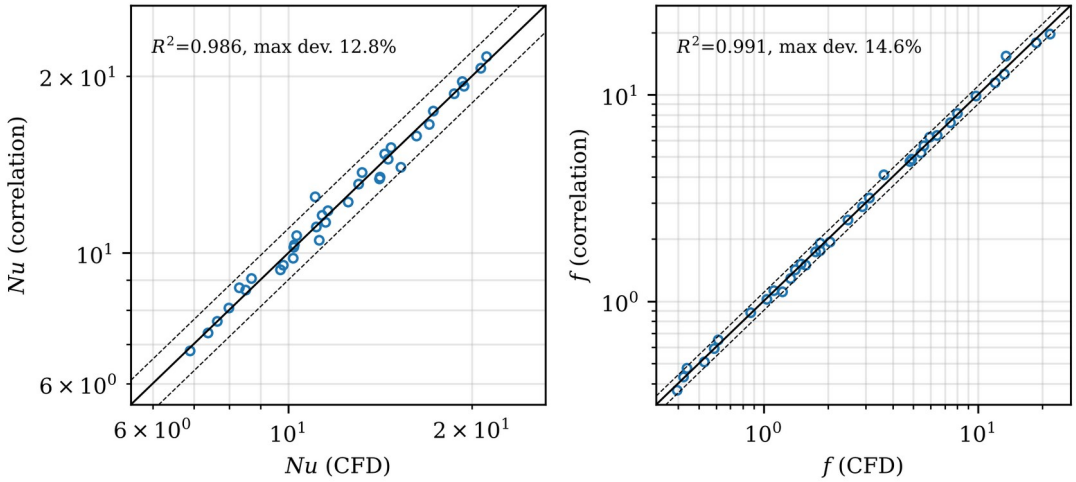


Fig. 6. Parity plots of (a) Eq. (10) and (b) Eq. (11) against the numerical results; dashed lines indicate ±10%.

7. LIMITATIONS

(i) The model is two-dimensional and represents channels much wider than they are high; side-wall effects and three-dimensional vortices are not included. (ii) The flow is laminar and steady; at higher Re or blockage, unsteady shedding would raise both Nu and f. (iii) The PV laminate is represented by a uniform heat flux; in practice, lateral conduction in the glass and cells smooths the temperature distribution, and the flux decreases as the module cools. (iv) The heated section is 10H long; a full module is longer, and the bulk-temperature rise along it, which baffles do not change, then dominates the module temperature. The temperature reductions in Section 5 are reductions of the wall-to-bulk difference and apply along the module only where the flow is periodically developed. (v) Buoyancy and radiation are neglected ($\mathrm{Ri_q} \leq 0.28$). (vi) The friction factor of the most blocked cases is underestimated by up to about 11% on the production grid (Section 3.2). (vii) Dust deposition on the channel inlet and baffles, which is common at agricultural sites, was not considered. (viii) The study is numerical, and an experimental test on a solar pumping array under Iraqi summer conditions is recommended before use in design.

8. CONCLUSIONS

(1) Adiabatic transverse baffles on the insulated wall of a narrow PV rear channel increase the average Nusselt number by 12–148% and reduce the maximum heated-wall temperature by 5–49% for 100 ≤ Re ≤ 600, mainly by deflecting the core flow onto the PV surface. Blockage is the dominant parameter; baffle number has a secondary effect.

This article is published under the terms of the **Creative Commons Attribution 4.0 International License (CC BY 4.0)**, which permits unrestricted use, distribution, and reproduction in any medium, provided the original work is properly cited.

Al-Furat Journal of Innovations in Agricultural Sciences (FJIAS)
ISSN: 2789-6773 | https://doi.org/10.46649/fjias.v2.si1.18
Vol. 2, Special Issue 1 (2026): ICSDCC 2026 – 3rd International Conference on Sustainable Development and Climate Change

(2) The friction factor rises by a factor of 1.6–38, more than the heat transfer, so the equal-pumping-power criterion PEC is below unity (0.67–0.96) in all cases and would reject every design.

(3) A net-energy analysis for a 5 mm channel under Baghdad summer conditions shows that the electrical gain from the lower module temperature exceeds the additional fan power in all cases. The net gain reaches 9.8 W m^{-2} (5.4% of the reference output) with $n = 7$ and $e/H = 0.7$ at Re = 100.

(4) The optimum blockage decreases as the flow rate rises: highly blocked baffles are best at Re ≤ 200, and $e/H = 0.5$ is best at Re = 600, where the net gain of $e/H = 0.7$ baffles nearly vanishes. Operating at low flow with high blockage is more energy-efficient than raising the flow rate in a smooth channel.

(5) Correlations (10) and (11) predict Nu and f with mean deviations of 2.7% and 3.7%. For cooling the PV arrays of solar irrigation pumps, net power rather than PEC should be used to select baffle geometries; a water-free air channel of this kind can recover part of the summer output loss without competing with irrigation for scarce water.

AUTHOR CONTRIBUTIONS

Jaber Ali Zghair: Conceptualization, Methodology, Software, Validation, Formal analysis, Visualization, Writing – original draft, Writing – review & editing.

FUNDING

This research received no external funding.

DECLARATION OF COMPETING INTEREST

The author declares no conflict of interest.

DATA AVAILABILITY STATEMENT

The solver source code and all computed fields are available from the corresponding author upon reasonable request.

REFERENCES

[1] Skoplaki, E. and Palyvos, J.A., 2009. On the temperature dependence of photovoltaic module electrical performance: a review of efficiency/power correlations. Solar Energy, 83(5): 614–624.

[2] Skoplaki, E. and Palyvos, J.A., 2009. Operating temperature of photovoltaic modules: a survey of pertinent correlations. Renewable Energy, 34(1): 23–29. https://doi.org/10.1016/j.renene.2008.04.009

[3] Hamad, A.J., 2020. Performance evaluation of polycrystalline photovoltaic module based on varying temperature for Baghdad city climate. Journal of Advanced Research in Fluid Mechanics and Thermal Sciences, 67(2): 164–176.

[4] Al-Akam, A., Abduljabbar, A.A. and Abdulhamed, A.J., 2024. Impact of different rooftop coverings on photovoltaic panel temperature. Energy Engineering, 121(12): 3762–3777. https://doi.org/10.32604/ee.2024.055198

[5] Chaichan, M.T., Kazem, H.A., Alnaser, N.W., Gholami, A., Al-Waeli, A.H.A. and Alnaser, W.E., 2021. Assessment cooling of photovoltaic modules using underground water. Arab Gulf Journal of Scientific Research, 39(2): 151–169.

This article is published under the terms of the **Creative Commons Attribution 4.0 International License (CC BY 4.0)**, which permits unrestricted use, distribution, and reproduction in any medium, provided the original work is properly cited.

Al-Furat Journal of Innovations in Agricultural Sciences (FJIAS)
ISSN: 2789-6773 | https://doi.org/10.46649/fjias.v2.si1.18
Vol. 2, Special Issue 1 (2026): ICSDCC 2026 – 3rd International Conference on Sustainable Development and Climate Change

[6] Salman, M.H., Obed, A.A. and Abid, A.J., 2021. Performance study of the direct-coupled photovoltaic water pumping system for the rural-isolated agricultural region in Iraq. Journal of Techniques, 3(1): 37–46. https://doi.org/10.51173/jt.v3i1.273

[7] Habeeb, W.H., 2018. Design and implementation of photovoltaic-water pumping system for use in Iraq. Journal of Engineering and Sustainable Development, 22(6): 141–151.

[8] Al-Hamdani, A.H., Hassan, M. and Ahmad, R.T., 2013. Optimal sizing of photovoltaic irrigation water pumping system in Samara. Engineering and Technology Journal, 31(16): 3067–3077.

[9] Badi, N. and Laatar, A.H., 2024. Improved cooling of photovoltaic panels by natural convection flow in a channel with adiabatic extensions. PLoS ONE, 19(7): e0302326. https://doi.org/10.1371/journal.pone.0302326

[10] El Kharaz, H., Khallaki, K., Kadiri, M.S. and Choukairy, K., 2024. A numerical analysis of air flow topology within a vertical channel attached behind photovoltaic panel. International Journal of Heat and Mass Transfer, 223: 125254. https://doi.org/10.1016/j.ijheatmasstransfer.2024.125254

[11] Moshfegh, B. and Sandberg, M., 1998. Flow and heat transfer in the air gap behind photovoltaic panels. Renewable and Sustainable Energy Reviews, 2(3): 287–301.

[12] Kelkar, K.M. and Patankar, S.V., 1987. Numerical prediction of flow and heat transfer in a parallel plate channel with staggered fins. Journal of Heat Transfer, 109(1): 25–30. https://doi.org/10.1115/1.3248058

[13] Henniche, R. and Korichi, A., 2025. Mixed and forced convection heat transfer in baffled channels: a brief review. Journal of Heat and Mass Transfer Research, 12(1): 15–28.

[14] Boonloi, A. and Jedsadaratanachai, W., 2023. Numerical investigations of laminar air flow and heat transfer characteristics in a square channel inserted with discrete X-V baffles (XVB). Frontiers in Heat and Mass Transfer, 21(1): 317–336. https://doi.org/10.32604/fhmt.2023.044929

[15] Lima-Téllez, T., Hinojosa, J.F., Hernández-López, I. and Moreno, S., 2024. Numerical study of the thermal performance of a single-channel cooling PV system using baffles and different nanofluids. Heliyon, 10(15): e35413. https://doi.org/10.1016/j.heliyon.2024.e35413

[16] Altharwanee, H., Jurado, F. and Vera, D., 2024. PV/T water-based cooling in hot climate conditions by using semi-circle baffles. International Journal of Power Electronics and Drive Systems, 15(4): 2660–2673. https://doi.org/10.11591/ijpeds.v15.i4.pp2660-2673

[17] Webb, R.L., 1981. Performance evaluation criteria for use of enhanced heat transfer surfaces in heat exchanger design. International Journal of Heat and Mass Transfer, 24(4): 715–726.

[18] Karwa, R., Sharma, C. and Karwa, N., 2013. Performance evaluation criterion at equal pumping power for enhanced performance heat transfer surfaces. Journal of Solar Energy, 2013: 370823. https://doi.org/10.1155/2013/370823

[19] Shah, R.K. and London, A.L., 1978. Laminar Flow Forced Convection in Ducts. Academic Press, New York, USA.

[20] van Leer, B., 1974. Towards the ultimate conservative difference scheme. II. Monotonicity and conservation combined in a second-order scheme. Journal of Computational Physics, 14(4): 361–370.

This article is published under the terms of the **Creative Commons Attribution 4.0 International License (CC BY 4.0)**, which permits unrestricted use, distribution, and reproduction in any medium, provided the original work is properly cited.